Performance Enhancement of the Guiding Apparatus in a Nozzle-Type Reaction Micro Hydropower Turbine

Sardor Mirzayev[1,2], Oybek Bozarov[3] and Isroil Yuldoshev[4]
[1]*Andijan Institue of Agriculture and Agrotechnologies, Oliygokh Str. 1, 170103 Andijan, Uzbekistan,*
[2]*National Research University "Tashkent Institute of Irrigation and Agricultural Mechanization Engineers", Kari Niyazov Str. 39, 100000 Tashkent, Uzbekistan*
[3]*Kokand University, Andijan Branch, Babur Shokh Str. 2-b, 170100 Andijan, Uzbekistan,*
[4]*Tashkent State Technical University named after Islam Karimov, Universitet Str. 2, 100095 Tashkent, Uzbekistan*
mirzayevsardor33@gmail.com, obozarov7@inbox.ru, yuldashev.i2004@gmail.com.

Keywords: Nozzle, Hydroturbine, Internal Flow-Guiding Apparatus, Computational Fluid Dynamics (CFD), Experimental Investigations, Micro-Hydropower Systems, Renewable Energy Technologies.

Abstract: The study addresses the utilization of low-pressure water sources for electricity generation as an important approach to ensuring sustainable energy supply in rural and remote areas. Conventional turbines experience high energy losses, frequent cavitation phenomena, and reduced service life under low-pressure conditions. To overcome these challenges, this research focuses on improving the internal guiding mechanism of a nozzle-type reactive micro-hydroturbine to enhance efficiency, minimize energy losses, and extend operational durability. The main objective is to design and develop a conical confusor-based internal guiding mechanism with optimized blades and to assess its influence on flow stability and efficiency through CFD modeling and experimental verification. The research employs a comprehensive methodology combining analytical analysis, mathematical modeling, and experimental testing. Bernoulli's equations were applied to determine flow velocity and energy losses, while CFD modeling was performed using COMSOL Multiphysics 6.1 software based on the RANS method with a k–ε turbulence model. Flow velocity and pressure distribution were analyzed, and a 500 W prototype of the hydroturbine was experimentally tested under 2–6 meters of water head on a specially designed laboratory stand. The results contribute to improving the performance and operational stability of micro-hydroturbines designed for low-pressure water sources, promoting the wider implementation of sustainable energy technologies in decentralized power systems.

1 INTRODUCTION

According to the International Energy Agency's 2024 report, the reserves of hydrocarbon fuels will historically last for a relatively short time; that is, if consumed at the current rate, natural gas and oil fuels are expected to last for 70–80 years, while coal may last for 150–200 years [1]. In this period of rapidly increasing global energy demand, saving underground fuel reserves and preventing environmental problems require the efficient use of all types of renewable energy sources to produce environmentally clean energy. Therefore, the effective utilization of existing low-head water resources in the field of hydropower, which is one of the renewable energy sources, can also contribute to solving the abovementioned issues. Electricity generation from low-head water resources, especially in rural and decentralized remote areas, can be considered both as a method of organizing power supply based on hydropower systems (rivers, irrigation canals, and small reservoirs) and as an ecological solution through the rational use of water resources. It is well known that when conventional turbines operate under low-head conditions, a number of problems arise. These include strong turbulence, uneven velocity distribution, cavitation, and significant energy losses due to local and hydraulic resistances, resulting in reduced turbine service life. In most hydroturbines, the efficiency does not exceed 70% [2]. Over the past decade, many researchers have worked on improving the performance of hydroturbines designed for low-head operation. This has been done by enhancing the runner wheels and guide vanes, optimizing the nozzle geometry in jet turbines, and improving the design of guide vane geometry [3]. In particular, studies on guide vane

control, turbulence reduction, cavitation mitigation, and overall efficiency improvement have been carried out. Hue L. et al. [4] emphasized that, under low-head conditions, the energy recovery efficiency with guide vanes could be improved by up to 3.11%. Bao Ngoc Tran et al. [5] found that, in guided vane configurations, a combination of eight vanes with a 30° inclination could increase efficiency by 6.3% and power output by 4.2%. Such modeling and CFD analysis results were also reported in the works of Ramalho, R. V. C. et al. [6] and Barsi, D. et al. [7], who showed that regulation of flow could improve hydraulic efficiency across a wide range of operating conditions. Chaulagain, R. K. et al. presented findings on the characteristics of existing turbines. In most cases, research results remain limited to CFD [8]; comprehensive methodologies combining analytical modeling, numerical simulations, and prototype testing have not been sufficiently applied. Furthermore, much of the literature is devoted to medium-scale systems of 20–500 kW, while compact prototypes below 5 kW have not been adequately studied. Yet, such systems are of crucial importance for rural agriculture and electrification of remote networks. Recent studies have analyzed, in detail, the influence of the number and shape of guide vanes as well as additional conical parts on hydraulic losses and overall energy performance using CFD software. For instance, Takamure et al. [9] investigated small hydroturbines with conical devices, determining torque and output power by comparing CFD and experimental results. Their findings confirmed the positive effect of diffusers on the flow process. Shi et al. [10], based on entropy theory, analyzed the effect of different guide vane numbers on energy losses, concluding that an increase in vane number leads to higher efficiency. Yang et al. [11] developed a novel "Split Sliding Guide Vane" (SSGV), which successfully eliminated leakages in the flow and improved system stability. Vijay Kumar et al. [12], by varying the opening degree of guide vanes in a Francis turbine, demonstrated that maximum efficiency depends on the opening angle (≈50.25%). This result provides a methodological basis for determining the turbine's optimal operating regime. Romero-Menko et al. [13] studied cross-flow turbines and showed that the shape and arrangement of internal elements and nozzle configuration significantly affect turbine efficiency. Similar results can be seen in other similar studies on low-head hydroturbines [14]-[17]. The literature review indicates that optimization of internal guide apparatus and CFD modeling contribute significantly to experimental validation. However, the application of conical diffusers and optimized vane geometries in jet hydroturbines has not yet been studied. The novelty of this research lies precisely in this aspect: the combined application of analytical modeling, CFD simulation, and experimental testing to justify the optimal parameters of a jet reaction turbine.

2 MATERIALS AND METHODS

The general scheme of the hydroturbine with an improved internal guiding structure is presented below (Fig. 1).

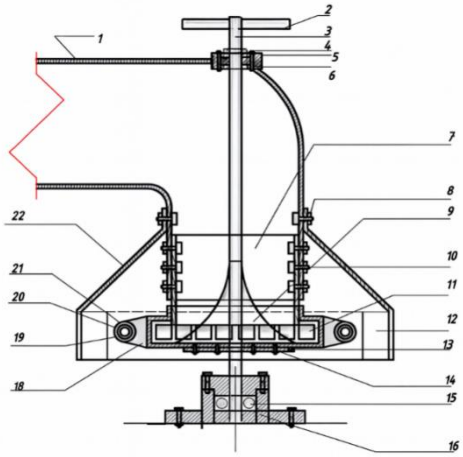

Figure 1: General scheme of the reaction hydroturbine with an improved internal guiding structure: 1 – water inlet channel; 2 – pulley; 3 – shaft; 4 – gland; 5 – bearing; 6 – bearing housing; 7 – supply cylinder of the improved internal guiding structure; 8 – stationary housing of the hydroturbine and fixing bolts; 9 – conical diffuser of the guide device; 10 – attachment bolts of the guide device to the supply pipe; 11 – guide vane profile; 12 – water-returning blades of the stator; 13 – runner cylinder; 14 – cylindrical base connecting the runner to the shaft; 15 – lower base bearing fixed to the dam; 16 – base bearing housing; 17 – platform; 18 – water inlet channel to the nozzle; 19 – nozzle working body; 20 – nozzle diffuser; 21 – water outlet channel and diffuser; 22 – stator of the hydroturbine.

The water flow, maintained at constant pressure in the reservoir, passes through supply pipe (1) into the supply cylinder (7) of the improved internal guiding structure. It then enters the gap between the central conical diffuser (9) and the supply cylinder, which gradually narrows towards the lower section. In this stage, the water flow, initially in the vertical direction, is smoothly redirected into the horizontally oriented guide vanes (11). During this transition, while the flow width remains constant, its direction changes

relative to the radial axis and acts upon the inner wall of the nozzle (18), which is fixed to the runner cylinder (13), at an optimized angle β = 15–18°.

At the nozzle inlet, the flow exerts pressure and active force on the inner surface. After reflecting from the inner wall of the nozzle, the water jet continues toward the diffuser section (20) of the outlet channel (19). The water jet exits the nozzle at high velocity in a compact stream, creating an impulse force in the opposite direction, which generates a reactive force on the nozzle. Consequently, the runner of the hydroturbine rotates in the opposite direction to the water jet. The outgoing jet strikes the vertically positioned stator blades (12) of the stator (22) perpendicularly, after which, under the influence of gravity and the inclination of the stator blades, the water falls downward and exits through the discharge channel. The rotary motion of the runner is transmitted to the generator via the shaft (3) connected to the pulley (2).

The motion of water inside the hydroturbine consists of several stages. Considering the energy loss due to nozzle type, a correction factor φ = 0.95 was introduced. The average velocity of water at the turbine inlet section (υ_1) was calculated using Bernoulli's equations, based on the mean flow velocity up to the entry point of the internal guiding structure vanes [17]:

$$\upsilon_2 = \sqrt{\frac{\frac{\rho Q \upsilon_1}{\gamma S_2}\left(\frac{S_1}{S_2}-1\right)+\frac{\alpha_1 \upsilon_1^2}{2g}-\sum h_{1i}+z_1-z_2}{\alpha_2}\cdot 2g}, \quad (1)$$

where F_d – cross-sectional area of water flow at the turbine inlet (minimum section); F – cross-sectional area of the supply pipe; υ_1 – average velocity at turbine inlet; Q – flow rate.

To analyze the motion of water through the internal guiding structure, the schematic diagram shown in Figure 2 was used.

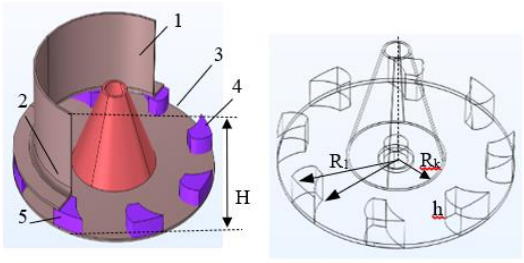

Figure 2: General schematic view of the improved internal guiding structure: 1 – supply cylinder; 2 – annular upper disc; 3 – lower disc; 4 – guide vanes; 5 – water outlet from the guiding structure.

Let υ_2 denote the average velocity of water exiting through the channels between discs (2) and (3). When the water is redirected from vertical to horizontal channels, energy losses occur due to the 90° turn and friction with the guide vanes. However, since vane dimensions are relatively small, frictional losses can be neglected. To ensure no energy loss when water flows from the supply cylinder to the nozzle, the cross-sectional area of the supply cylinder (S_2, with diameter d_2) must equal the total inlet area of the channels. The channels are placed symmetrically along the cylinder periphery. Assuming all dimensions are identical, the vane height H_k is determined by:

$$H_k = \frac{\pi d_2}{2k\varphi\alpha}, \quad (2)$$

$$\varphi = \frac{\alpha d_2 - \delta}{\alpha d_2}, \quad (3)$$

where k – number of vanes; φ – flow coefficient at vane entrance; α – central angle between adjacent vanes; δ – sum of vane thickness and blocked arc length for fixing.

Based on Zhukovsky's theory, the velocity of water exiting the guiding structure is given by:

$$\upsilon_3 = \upsilon_2\left(\frac{kl\sin\alpha_1}{d_2}+\cos(\alpha_2-\alpha_1)\right) \quad (4)$$

where l – vane length; α1, α2 – entry and exit angles of the guide vanes.

The total energy loss of the water flow in the turbine is determined as:

$$h_G = \left(\frac{S_1}{S_2}-1\right)^2\frac{\upsilon_1^2}{2g}+\xi_{90^\circ}(1-\cos\varphi_2)\frac{\upsilon_3^2}{2g}+\xi_{SK}\frac{\upsilon_3^2}{2g}+\left(\frac{S_3}{S_6}-1\right)^2\frac{\upsilon_4^2}{2g} \quad (5)$$

where ξ – hydraulic resistance coefficient; α – cone formation angle; ψ – proportionality coefficient (ψ = 2 for pipes, ψ = 1 for rectangular sections); λ – Darcy friction coefficient.

The torque and angular velocity of the runner were determined using the general theorem on the variation of angular momentum for a rigid body:

$$\omega_z = \frac{S_3\upsilon_3^2\left(\cos\beta+\sqrt{\frac{S_3}{S_6}\left(\frac{S_3}{S_6}-1\right)+1-\frac{1}{2}\left(\xi_{SK}+\xi_{90}\right)}\right)}{\pi r_c^3\upsilon_4}+\frac{\upsilon_4}{r_c}; \quad (6)$$

where r_c – distance from the rotation axis to nozzle center; υ_3, υ_4 – water velocities at nozzle inlet and outlet.

Table 1: Parameters introduced in mathematical modeling.

Name	Expression	Value	Description
dens	1000[kg/m^3]	1000 kg/m³	Water density
visc	8.9e-4[Pa*s]	1E−5 Pa·s	Dynamic viscosity of water
vs	6[m/s]	6 m/s	Water inlet velocity into the nozzle
Re	2*R1*vs*dens/visc		Reynolds number
Q	0,2[m^3/s]	0,2 m³/s	Water flow rate
H	2,5 [m]	2,5 m	Static head of water
omega z	6,6 [rad/s]	6,6 rad/s	Angular velocity of the runner
bm	0,004[m]	0,004 m	Thickness of the nozzle wall
alfa1	15[grad]	0,2618 rad	Water inlet angle to runner guide vane
alfa2	12[grad]	0,20944 rad	Water outlet angle from runner guide vane
betta	15[grad]	0,2618 rad	Installation angle of the guide vane relative to radial direction
lamb	0,05	0,05	Darcy friction coefficient
G	9,81[m/s^2]	9,81 m/s²	Gravitational acceleration
N	8	8	Number of guide vanes
fi_0	0,95	0,95	Water inlet coefficient
hi	15[grad]	0,2618 rad	Diffuser angle at nozzle outlet
R_1	(Q/(3,14*fi0*(2*g*H)^0,5))^0,5	0,10346 m	Inlet pipe radius to hydroturbine
R_2	0,98*R1	0,10139 m	Radius of supply cylinder in guiding device
myu	S3/S4	3	Ratio of inlet to outlet areas of nozzle
delta	0,02[m]	0,02 m	Distance between runner cylinder and guide vane
Hk	0,026[m]	0,026 m	Radial height of the guide vane
m	4	4	Number of nozzles
Rs	Hk + delta + bm + R2	0,15139 m	Distance from runner center to nozzle
p	10	10	Percentage of circle occupied by nozzle fixing
alfa	2*pi/m*n[deg]	0,21932 rad	Nozzle occupied angle
v_2	(fi0/R2^2)*(2*g*H*(R1^4 - R1^2*R2^2 + R2^4))^0,5	6,0774 m/s	Velocity of water at guide vane inlet
Lk	R2/myu	0,033796 m	Guide vane length
v_3	(Lk*m*v2*sin(alfa1)*cos(alfa2 - betta))/(2*R2) + v2*cos(alfa2 - alfa1)	7,1162 m/s	Velocity of water at nozzle inlet
L	Q/((1 - p/100)*Rs*v3*2*3,14/m)	0,13139 m	Vertical height of nozzle
S_3	2*3.14*Rs*(1 - p/100)*L/m	0,028105 m²	Nozzle inlet area
S_4	S3/2,5	0,011242 m²	Nozzle outlet area
eps_k	0.125*lamb*(1 - (S4/S3)^2)	0,00525	Energy loss coefficient in nozzle
sig	(d*(d - 1) + 1 - (eps_k + 1.25)/2)^0.5	2.0304	Intermediate calculation coefficient
v_4	v3*sig	14,449 m/s	Velocity of water at nozzle outlet
c	S3*v3^2*(sin(betta + sig))/(3.14*v4)	0,023557 m³/s	Defined coefficient
Rshould d	1.7*Rs	0,25736 m	Arm of force

The energy parameters of the hydroturbine were analyzed using mathematical modeling. CFD simulations were carried out in COMSOL Multiphysics 6.1 (CFD module), applying the standard RANS method and the "Turbulent Flow, k-ε" model for five different guide vane and cone geometries. The velocity and pressure variations of water at different points of the nozzle were studied through mathematical modeling depending on nozzle geometry and number. This model achieves high accuracy in calculating Reynolds shear stresses and tensors for low-head flow gradients.

The dimensions and parameters of the small experimental hydroturbine used for simulation and laboratory testing are presented in Table 1.

3 RESULTS AND DISCUSSIONS

Figures 3 and 4 illustrate the changes in velocity and pressure fields of the hydraulic reaction turbine for both the conventional (non-improved prototype) and the improved internal guiding structures.

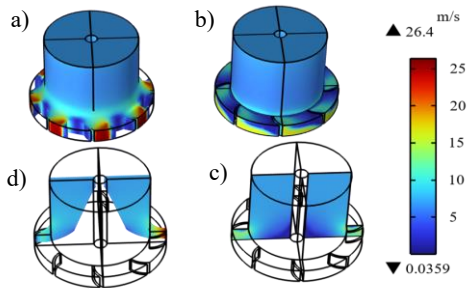

Figure 3: Analysis of water flow velocity field in hydroturbine guide devices: (a) 3D view of water flow in the improved guiding device; (b) 3D view of water flow in the conventional device; (c) water flow characteristics in the XOZ plane of the improved guiding device; (d) water flow characteristics in the XOZ plane of the conventional guing iddevice.

As can be seen from Figure 3, in the conventional turbine (right), multiple red and yellow zones (~20–26) are present around the device. These zones indicate strong turbulence, vortices, or regions of flow acceleration and deceleration. Particularly between the lower vanes, strong flow irregularities and energy losses are observed. In the improved turbine (left), the color gradient is smoother, dominated by blue and green areas (~5–15), which reflects a more stable flow - laminar or optimally turbulent. The flow is more centralized with fewer vortices and reduced turbulence.

Focusing on the inter-vane flow, in the conventional turbine, high-velocity regions in the lower section change abruptly, producing swirling motions inside the flow that generate additional resistance and reduce efficiency. In contrast, in the improved turbine, the inter-vane flow is more centralized and smoother. This condition indicates reduced energy losses and better conversion of flow energy into mechanical energy, attributed to minimized heat losses and vortex formation in the improved design.

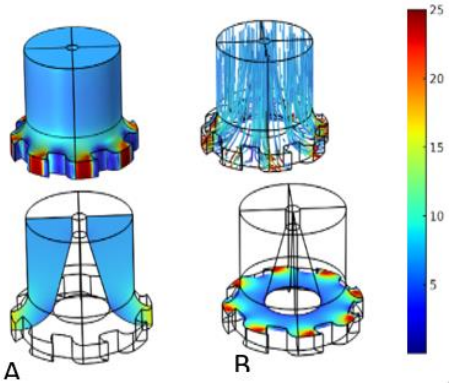

Figure 4: Fluid interaction in the improved internal guiding device of the hydroturbine: (A) velocity distribution; (B) pressure distribution.

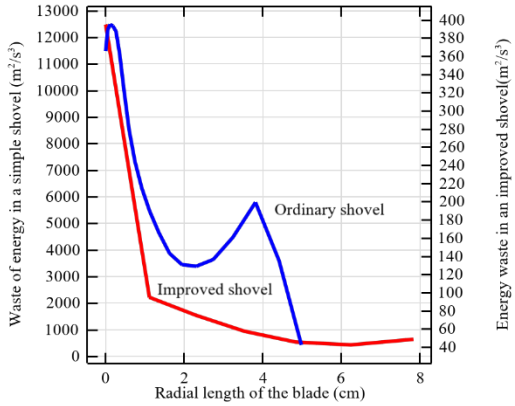

Figure 5: Energy losses due to turbulence in conventional and improved guiding devices with vanes.

From the pressure distribution analysis shown in Figure 4, it is evident that in the conventional guiding device, the water jet exiting the window expands and produces a vortex-like motion, leading to significant energy dissipation due to eddies and sudden expansion. This reduces the torque applied to the runner. In contrast, in the improved guiding device, the water flow passes through the guiding window without changing the spacing between the vanes,

directed toward the nozzle walls, producing maximum torque on the runner. The properly aligned and accelerated jet towards the nozzle walls increases turbine efficiency.

As illustrated in Figure 5, comparison of the flow zones between conventional and improved vane-type hydroturbines reveals the following observations:

- In the initial zone (0 – 1.5 cm), the turbulence dissipation rate is very high (~5000+ m^2/s^3) for the conventional vane design (blue), whereas in the improved vane design (red/green), turbulence and energy dissipation are significantly lower. The smoother acceleration of the flow in the improved vane reduces energy losses.
- In the middle zone (1.5 – 6 cm), turbulence sharply decreases (from 5000 → ~1000 m^2/s^3), indicating rapid attenuation of instability in the flow. The improved vane maintains flow stability over a longer distance, which enhances aerodynamic efficiency and reduces system friction.
- In the final zone (6 – 13 cm), the velocity in the conventional vane device drops considerably (~9 m/s), while in the improved vane device, velocity remains higher (~10–11 m/s). This demonstrates that energy is dissipated more slowly.

Thus, in the improved vane design, the flow remains more stable and energy-rich, ensuring improved heat transfer and higher driving power. Due to reduced turbulence and sustained high velocity, cavitation decreases, and the service life of the turbine is nearly doubled.

A small-scale model of the hydroturbine was fabricated and tested experimentally. The experimental results were compared with those of the conventional prototype.

It was found that there are almost no dedicated stands available for testing small-scale hydroturbine models; existing stands are large in size, equipped with outdated components, and suitable for testing only one or two turbine types with limited capability to vary water head and flow rate. Moreover, constructing a new turbine prototype for such stands requires significant financial costs.

Therefore, a test stand was developed that allows experimental studies of various pico-hydroturbine prototypes, along with a testing methodology (Fig. 6).

The fabricated stand has the following structure: a frame with two reaction hydroturbines installed, supplied with water through three low-pressure pumps (1.5 kW each). The inlet water pressure of the hydroturbine is monitored using four manometers. The rotary motion from the turbine shaft is transmitted via a pulley to a generator, with a transmission ratio of 2.2. The generated electricity is supplied to a specially designed transformer. The transformer output, including current and voltage, is measured and displayed on a control panel. As a load, two 50 W lamps and a 150 W resistance coil were used. The generated current and voltage were measured using Class A ammeters and voltmeters.

Figure 6: Experimental setup of the improved micro-hydroturbine model.

The water flow rate and pressure were regulated by controlling the rotational speed of the pumps using a frequency regulator, with the range varying from 0 to 5000 rpm. Additionally, water circulation before the pump was provided through valves to extend the range of flow and pressure control.

The small-scale nozzle-type reaction hydroturbine model was tested on this stand. During the experiments, water pressure at different points in the turbine was measured using manometers, the water flow rate was determined from a calibrated scale in the measuring tank, and the runner's rotational speed was measured using a tachometer.

The analytical, numerical, and experimental investigations conducted in this study demonstrate that the proposed internal guiding device - consisting of a diffuser cone and optimized guide vane geometry - significantly improves the performance of nozzle-type reaction turbines under low-head conditions.

Compared with the conventional design, the efficiency of the improved turbine reached 85.5%, which is 3.4% higher than that of the conventional turbine (82.1%). This increase in efficiency primarily results from two mechanisms: (i) the conical diffuser stabilizes the inlet flow to the guide vanes, reducing turbulence and secondary vortices; and (ii) the optimized guide vane geometry minimizes hydraulic losses and enhances energy transfer to the shaft.

In addition, the maximum rotational speed increased by almost 14%, confirming the enhancement of energy efficiency.

A comparison of analytical, CFD, and experimental results further supports these findings. Analytical evaluation showed an efficiency of 86.2%, CFD simulations yielded 86.6%, and experimental measurements recorded 85.5%. The close agreement between these values demonstrates the reliability of the proposed design and the validity of the adopted methodology. A deviation of less than 1.5% confirms that CFD, when supported by analytical theory and validated through experiments, can serve as an effective predictive tool for turbine optimization.

From a practical standpoint, the improved turbine is particularly well suited for rural electrification and irrigation canal systems, which are widely implemented in Uzbekistan and other developing countries. By reducing the risk of cavitation and extending the service life of the turbine by approximately 50–55%, the design not only enhances efficiency but also decreases maintenance costs and downtime, thereby improving overall economic feasibility.

4 CONCLUSIONS

This study focused on the improvement of the internal guiding device of a nozzle-type reaction turbine under low-head conditions through CFD modeling and experimental testing. The novelty of the work lies in the use of a conical diffuser and optimized guide vane geometry to control flow, reduce hydraulic energy losses, and enhance both efficiency and turbine service life.

The research employed analytical evaluation of flow, velocity, torque, and efficiency; CFD simulations using the RANS approach with the k–ε turbulence model in the COMSOL Multiphysics platform; and experimental testing of a 500 W prototype on a specially designed laboratory stand with an adjustable water head of 1.5–6 meters.

The results provided new scientific insights into the influence of internal guiding devices on turbine performance. The improved design reduced hydraulic losses by 35–40%, increased efficiency from 82.1% to 85.5%, and extended turbine service life by approximately 50–55%.

ACKNOWLEDGMENTS

The author would like to express sincere gratitude to Prof. Dr. R. Aliyev of Andijan State University for his valuable guidance, constructive suggestions, and support throughout the research process.

This work was financially supported by Kokand University, Andijan Branch, Uzbekistan.

REFERENCES

[1] International Energy Agency, World Energy Outlook 2024. [Online]. Available: https://iea.blob.core.windows.net/assets/140a0470-5b90-4922-a0e9-838b3ac6918c/WorldEnergyOutlook2024.pdf.

[2] B. N. Tran, B. G. Kim, and J. H. Kim, “The effect of the guide vane number and inclined angle on the performance improvement of a low head propeller turbine,” Journal of Advanced Marine Engineering and Technology, vol. 45, no. 4, pp. 205–212, 2021.

[3] O. Bozarov, R. Aliyev, D. Kodirov, D. Bozorov, and S. Saidullaeva, “Analysis of the efficiency of a counter-rotary hydraulic unit with a jet hydro turbine based on a Segner wheel,” E3S Web of Conferences, vol. 497, 01017, 2024, doi: 10.1051/e3sconf/202449701017.

[4] L. Xue, B. Cui, Z. Zhu, R. Wang, Z. Yang, J. Hu, and X. Su, “Effect of the guide vane on the hydraulic stability of a low-head, large-discharge industrial hydraulic turbine,” Journal of Applied Fluid Mechanics, vol. 17, no. 3, pp. 713–725, 2024, doi: 10.47176/jafm.17.3.2056.

[5] B. N. Tran, B. G. Kim, and J. H. Kim, “The effect of the guide vane number and inclined angle on the performance improvement of a low head propeller turbine,” Journal of Advanced Marine Engineering and Technology, vol. 45, no. 4, pp. 205–212, 2021.

[6] R. V. C. Ramalho et al., “Design of low-cost axial-flow turbines for very low-head micro-hydropower plants,” Processes, vol. 13, no. 6, p. 1865, 2025, doi: 10.3390/pr13061865.

[7] D. Barsi, R. Fink, P. Odry, M. Ubaldi, and P. Zunino, “Flow regulation of low head hydraulic propeller turbines by means of variable rotational speed: Aerodynamic motivations,” Machines, vol. 11, no. 2, p. 202, 2023, doi: 10.3390/machines11020202.

[8] R. K. Chaulagain, L. Poudel, and S. Maharjan, “A review on non-conventional hydropower turbines and their selection for ultra-low-head applications,” Heliyon, vol. 9, no. 7, e17753, 2023, doi: 10.1016/j.heliyon.2023.e17753.

[9] K. Takamure, T. Uchiyama, K. Horie, and H. Nakayama, “Effect of cone on efficiency improvement of self-powered IoT-based hydroturbine,” Advances in Mechanical Engineering, vol. 14, no. 7, 2022, doi: 10.1177/16878132221107249.

[10] F. Shi, D. Zhang, P. Wang, X. Wang, and C. Feng, “Analysis of energy loss mechanism in hydraulic turbines with different directional blades based on entropy generation theory,” Processes, vol. 13, no. 6, p. 1899, 2025, doi: 10.3390/pr13061899.

[11] D. Yang, K. Wang, X. Wang, Q. Zhang, X. Lei, and L. Xu, “Performance and internal flow investigation of variable nozzle turbines with separable sliding guide vanes,” Machines, vol. 10, no. 11, p. 1084, 2022, doi: 10.3390/machines10111084.

[12] V. Kumar et al., “Experimental investigation and performance characteristics of Francis turbine with different guide vane openings in hydro-distributed generation power plants,” Energies, vol. 15, no. 18, p. 6798, 2022, doi: 10.3390/en15186798.

[13] F. Romero-Menko, J. Pineda-Agirre, L. Velasquez, A. Rubio-Clemente, and E. Chica, “Effect of nozzle configuration with and without internal guide vanes on the efficiency of small cross-flow hydroturbines,” Processes, vol. 12, no. 5, p. 938, 2024, doi: 10.3390/pr12050938.

[14] T. Sudsuansee, S. Phitaksurachai, R. Pan-Aram, N. Sritrakul, and Y. Tiaple, “Design and hydrodynamic performance of a low-head propeller hydroturbine for high-efficiency operation over a wide range,” International Journal of Thermofluids, vol. 27, p. 101228, 2025, doi: 10.1016/j.ijft.2025.101228.

[15] S. Bozhinova, V. Hecht, D. Kisliakov, G. Müller, and S. Schneider, “Hydropower converters with head differences below 2.5 m,” Proceedings of the Institution of Civil Engineers – Energy, vol. 166, no. 3, pp. 107–119, 2013, doi: 10.1680/ener.11.00037.

[16] E. T. Woldemariam, H. G. Lemu, and G. G. Wang, “CFD-driven valve shape optimization for improving the performance of a micro cross-flow turbine,” Energies, vol. 11, no. 1, p. 248, 2018, doi: 10.3390/en11010248.

[17] O. Bozarov, R. Aliev, I. Yuldashev, N. Kozimjonov, and S. Saidullaeva, “Results of mathematical modeling of the nozzle of the counter-rotor hydraulic unit,” AIP Conference Proceedings, vol. 3152, no. 1, 040019, Jun. 2024, doi: 10.1063/5.0220058.